DEGREE PROGRAMME IN WIRELESS COMMUNICATIONS ENGINEERING

MASTER'S THESIS

VALIDATION OF MEASUREMENT SETUP FOR ASSESSING COMPLEX DIELECTRIC CONSTANT

Author	Pankaj Chakrabarty
Supervisor	Risto Vuohtoniemi
Second Examiner	Markus Berg
Technical Advisor	Veikko Hovinen

December 2019

Chakrabarty P. (2019) Validation of Measurement Setup for Assessing Complex Dielectric Constant. University of Oulu, Faculty of Information Technology and Electrical Engineering, Degree Programme in Wireless Communications Engineering. Master's Thesis, 43 p.

ABSTRACT

Electromagnetic waves interact with different obstacles or materials. The propagation of electromagnetic waves depends on how they interact with different materials. Understanding the transmission and reflection characteristics of various media leads to understanding the propagation of electromagnetic waves. The transmission and reflection of radio waves are dictated by the dielectric properties of the material. The estimation of dielectric properties of a material is acquired by proper measurement techniques and methods. In this thesis, a measurement setup for assessing complex dielectric constant is verified. The measurement setup is designed with two high frequency horn antennas and a two-port vector network analyzer, controlled by a computer via a GPIB interface. Various measurement scenarios and results needed to achieve the goal are presented in the thesis. All measurements are done in an anechoic chamber. The measurement data is collected in frequency ranges of 1-9.5 GHz and 9.5-18 GHz. Furthermore, reflection measurements are taken from the side wall absorbers in the same anechoic chamber for checking the wall absorption characteristics. The key findings of this experiment are dielectric constant, Brewster angle and the reflection coefficient. The obtained value of the dielectric constant can be further used for similar type of environments or measurement setup.

Key words: electromagnetic waves, dielectric constant, vector network analyzer, anechoic chamber.

TABLE OF CONTENTS

ABSTRACT 2
TABLE OF CONTENTS 3
FOREWORD 5
LIST OF ABBREVIATIONS AND SYMBOLS 6
1. INTRODUCTION 9
2. PROPAGATION MECHANISMS 11
2.1. Nature of propagation 11
2.1.1. Line-of-sight propagation 11
2.1.2. Non-line-of-sight propagation 12
2.2. Affected phenomena during propagation 12
2.2.1. Reflection 12
2.2.2. Refraction 13
2.2.3. Diffraction 15
2.2.4. Absorption 15
2.2.5. Polarization 15
2.2.6. Scattering 17
2.2.7. Path loss 18
2.2.8. Multipath fading 19
3. COMPLEX DIELECTRIC CONSTANT 20
3.1. Definition of dielectric constant 20
3.2. Effect of dielectric constant 20
3.3. Interaction in boundary of two medium 21
4. CHANNEL MODELLING 22
4.1. Tapped delay line model 22
4.2. Indoor channel models 23
4.3. MIMO channel models 23
5. MEASUREMENT TECHNIQUES 25
5.1. Channel measurement methods 25
5.1.1. Ultra-wideband channel sounding 25
5.1.2. Millimeter and submillimeter-wave systems 26
5.2. Measurement techniques for dielectric properties 26
5.3. VNA based measurement system 27
5.3.1. Proposed measurement system 27
5.3.2. Measurement setup 28
5.3.3. Antennas 29
5.3.4. Scattering parameters 29
5.3.5. Calibration 29
6. RESULTS AND ANALYSIS 31
6.1. Verification of the measurement setup 31
6.2. Sample measurement of the selected frequency ranges 31

6.3. Analysis of the measurement results 32
7. DISCUSSION 39
7.1. Evaluation of the proposed model 39
7.2. Possible improvements for future work 39
8. SUMMARY 40
9. REFERENCES 41

FOREWORD

It is often said that character is the lighthouse of success making small numbers formidable and procuring success and excellence in all orders. Succeeding in completing the thesis would not have been possible without the sheer cooperation, encouragement and support from people at all stages of this formative journey.

Firstly, I would like to extend my sincere gratitude to my technical advisor M.Sc (Tech.) Veikko Hovinen for his undeterred guidance. I would also like to sincerely thank my supervisor Lic.Sc (Tech) Risto Vuohtoniemi for leading me through thick and thin, helping me choose the right path and take the right decisions whenever required. I am also grateful to D.Sc (Tech) Markus Berg for reading and reviewing the thesis paper.

This work would not have been possible without the dedicated support and inspiration of Aviroop Mukherjee who never, for a moment failed to respect me as a true friend and give me company and keep my patience.

This thesis work has been performed as a requirement for the fulfilment of my Master's Degree Programme in Wireless Communication Engineering, at the Centre for Wireless Communication, University of Oulu, Finland. Finally, I would like to extend my warm regards and thanks to my brother Pijush Chakrabarty who always had my back with his solid belief and confidence and to my friends and family for their constant support and motivation. I sincerely dedicate this thesis work to my late father Paresh Chakrabarty and my mother Archana Chakrabarty who have always sacrificed themselves to fulfil my demands and last but not the least, I am grateful to the Almighty for making me capable enough to reach this stage where I am able to realize the fruitful end result of my efforts.

Oulu, Finland December 09, 2019

Pankaj Chakrabarty

LIST OF ABBREVIATIONS AND SYMBOLS

AWGN	additive white Gaussian noise
CAD	computer-aided design
DUT	device under test
FIR	finite impulse response
FM	frequency modulation
FMCW	frequency modulation continuous wave
FSPL	free space path loss
GPIB	general purpose interface bus
HF	high frequency
LAN	local area network
LHC	left hand circular
LO	local oscillator
LOS	line of sight
MBLS	maximum length binary sequence
MIMO	multiple input multiple output
mmW	millimeter-wave
MUT	material under test
NLOS	non-line of sight
PN	pseudo-noise
RF	radio frequency
RHC	right hand circular
RMSE	root-mean-square-error
RX	receiver
S-parameters	scattering parameters
TCP/IP	transfer control protocol/internet protocol
TDL	tapped delay line
TE	transverse electric
TEM	transverse electromagnetic
TX	transmitter
VNA	vector network analyzer
UHF	ultra-high frequency
UWB	ultra-wideband
VHF	very high frequency
VSWR	voltage standing wave ratio

a	surface area of dielectric sphere
a_1	incidence power at port 1
a_2	incidence power at port 2

A_1, A_2	samples of TDL
A_{R}	effective area of the surface of sphere
A_{T}	effective area of the transmitting antenna
b_0, b_1	delays of TDL
b_1	reflected power at port 1
b_2	reflected power at port 2
$\boldsymbol{B}$	magnetic field
C	capacitance
c	velocity of wave
c_0	wave velocity of vacuum
d	radius
d_{los}	length of LOS path
d_{refl}	length of reflected path
D	radius of the Earth
e_{x}	wave polarization in x direction
e_{y}	wave polarization in y direction
$\boldsymbol{E}$	electric field
$\boldsymbol{E}_i$	incidence electric field
$\boldsymbol{E}_r$	reflected electric field
f	frequency
G_{R}	receive antenna gain
G_{T}	transmit antenna gain
h	height of the antenna
$\boldsymbol{H}$	channel matrix
I_θ	intensity at a given angle
I_0	original intensity
L	number of taps
M	number of TX antennas
n_1	refractive index of medium 1
n_2	refractive index of medium 2
$n(t)$	additive white Gaussian noise
N	number of RX antennas
P	total power
P_{D}	radially directed power
P_{R}	total received power
P_{s}	scattered power form a dielectric sphere
P_{T}	total radiated power
Q	quality factor
$\boldsymbol{S}$	Poynting vector
S	power density
s_{11}	input port reflection coefficient
s_{12}	reverse gain

s_{21}	forward gain
s_{22}	output port reflection coefficient
$s(t)$	transmitted signal
t	time
v	material velocity
w	width of the aperture
x	distance to the radio horizon
$x(n)$	input signal of TDL
$y(n)$	output signal of TDL
$y(t)$	received signal

ε	permittivity
ε_0	permittivity of vacuum
ε_1	permittivity of medium 1
ε_2	permittivity of medium 2
ε_r	relative permittivity
η	wave impedance
η_0	wave impedance of vacuum
θ	zenith angle
θ_1	incidence angle
θ_2	refracted angle
θ_b	Brewster angle
θ_{min}	angle of minimum intensity
λ	wavelength
μ	permeability
μ_0	permeability of vacuum
μ_1	permeability of medium 1
μ_2	permeability of medium 2
μ_r	relative permeability
ρ	reflection coefficient
σ_s	ratio of the total scattered power
ω	angular frequency

1. INTRODUCTION

Radio technology used electromagnetic waves for transmission and detection in a straight line or by reflection [1]. Generally, for radio communication microwave bands are used but its need to increase bandwidth of the communication to fulfil the demand of various applications, e.g., artificial intelligence, internet of things, virtual reality, high definition video. In millimeter-wave (mmW) there is huge availability of bandwidth thus, mmW becomes the researchable topic for radio communications.

Though for emerging applications and demands increasing of bandwidth is highly needed, and mmW is the greatest solution for that, but there are some challenges communicating via mmW. It suffers from attenuation badly. The signal strength can be reduced due to gas, rain, and humidity absorption. Millimeter-waves have very short in wavelength and they are suitable for short range communication, and usually line of sight communication is needed. The nature of propagation of electromagnetic waves depends on the transmission and reflection characteristic form different materials in the environment. Thus, dielectric constant plays an important role in such communication. The key concern of this thesis is to arrange and verify a measuring setup to find out the complex dielectric constant of a plywood samples. A communication link has been created and measuring data are collected in frequency range 1-18 GHz by using vector network analyzer (VNA). VNA is a good instrument for this kind of setup. The setup is very simple because here only one TX antenna and one RX antenna are needed. It is possible to move the position and angle of the antenna to utilize a VNA based measurement system successfully, phase stability and length of the measurement cables play an important role. Another drawback of VNA is that it needs more sweep time proportional to number of measurement points. It is obvious that the throughput is going higher as much as the number of measurement points is lower, but the larger number of measurement points give higher trace resolution [2].

Many researchers had showed their interest in measuring dielectric constant and measured different dielectric materials. These researches and their findings give efficient techniques and methods to characterize the dielectric properties. A free-space measurement technique for estimating the complex dielectric is presented in [3]. The measurement process is done by using two horn antennas and a VNA. To estimate the dielectric properties of various walls at frequency range of 0.7-7 GHz, an oblique reflection model is implemented in [4]. The measurement setup is completed by a four-port vector network analyzer and two wideband dual-polarized cross-shaped antennas. Two 8 m long coaxial cables are also used. Measurements for parallel and perpendicular polarizations are obtained respectively by using the dual-polarized antennas. Time-domain gating is applied to separate the desired reflection and to suppress the line-of-sight component from the delayed response. Reference [5] has used pseudo-Brewster angle for measuring dielectric constant. In their experiment, two horn antennas are used to transmit and receive p-polarized waves. A dielectric sheet is located between the two antennas and rotated, which produces two peaks in the transmittance curves. From the curve the reflection coefficient is measured and thus the dielectric constant is achieved.

This thesis firstly gives the concept and aim of the whole work including some related works to this paper in chapter 1. Chapter 2 explains the nature of electromagnetic wave propagation and its properties. Chapter 3 gives the idea of dielectric constant and its effect. In chapter 4, discussion of channel modelling is presented, and chapter 5 elaborates about the measurement techniques. Chapter 6 presents the results

of the experiments and the analysis which established that the results are valid. Chapter 7 is based on the evaluation of proposed model and possible improvements in future. The whole work and concept are summarized in chapter 8, and finally, chapter 9 holds the references that are used during the study.

2. PROPAGATION MECHANISMS

This chapter discuss about the propagation nature of an electromagnetic wave and the challenges during propagation. The electromagnetic waves do not need a medium to transfer their energy from one location to another like mechanical waves do. It can travel through the vacuum, but in our real world the propagation electromagnetic waves can affected by different obstacles.

2.1. Nature of propagation

Electromagnetic waves are created by moving electrons. Maxwell's equations explain the propagation of electromagnetic waves, which denote that a changing magnetic field produces an electric field and vice-versa [6]. This is responsible for the self-propagation of electromagnetic waves. Connecting antennas to an electrical circuit, the electromagnetic wave can be transmitted efficiently, and a receiver can receive it from some distance.

2.1.1. Line-of-sight propagation

When signals are transmitted and received by a transmitter and a receiver without any type of obstacle between them is known as line-of-sight communication. FM radio, microwave and satellite transmission, etc. are examples of line-of-sight communication. Electromagnetic waves that are travelling in free space are propagating outward from the source in all directions, resulting in a spherical wavefront. These kinds of sources are called isotropic radiators, and which do not exist in the real world. The antenna polarization at the receiving end may ideally be like the polarization of the received wave. Similarly, the polarization of a transmitted wave is the same as that of the antenna from which it produced a vector cross product [7]. The vector cross product of an electric ($\boldsymbol{E}$) field and a magnetic ($\boldsymbol{B}$) field at any point indicates the direction of power flux at that point

$$\boldsymbol{S} = \boldsymbol{E} \times \boldsymbol{B} \, . \tag{1}$$

This cross product is known as the Poynting vector. By dividing this Poynting vector with the characteristic impedance of free space, one can get the resulting vector which gives both the direction of propagation and the power density. Consider the surface of an imaginary sphere surrounding the RF source than the power density can be expressed as

$$S = P/(4\pi d^2) \, , \tag{2}$$

where P is the total power at the source, d is the radius of the imaginary sphere and S is the power density on the surface of the sphere in $\mathrm{W/m^2}$ or equivalent. From (2), it seems that the power density of the electromagnetic wave is inversely proportional to d^2. The velocity of an electromagnetic wave depends upon the medium. In a vacuum,

the velocity of the electromagnetic wave is approximately $c = 3 \cdot 10^8$ m/s. The velocity of the electromagnetic wave through the air is very close to that of vacuum, and the same value is generally used. The distance traversed by the wave over one cycle (period) is determined as wavelength and it is generally denoted by the lambda

$$\lambda = c/f \ , \tag{3}$$

where *f* is the frequency.

2.1.2. Non-line-of-sight propagation

There exist several types of electromagnetic wave propagation except LOS propagation. Non-LOS propagation depends on the operation frequency. Non-LOS propagation describes terrestrial propagation where the transmitter and receiver have an obstacle between them. Meaningful communication can take place when reflection from and diffraction around buildings and foliage may provide enough signal strength. The effectiveness of indirect propagation is depended upon the amount of margin in the communication link and the signal strength of the reflected or diffracted signals. Frequencies from HF to UHF penetrate buildings and significant foliage quite simply. On the other hand, VHF and UHF will have a greater tendency to diffract around or reflect/scatter from the objects in the path. The obstruction tends to reflect or diffract the waves instead of scattering it when its options are compared to wavelength.

2.2. Affected phenomena during propagation

2.2.1. Reflection

Reflection refers to the direction change of a wave-front at the interface within two different media, thus it returns or bounces back towards the medium from which it originated. Radio waves are usually reflected from the ground and objects such as buildings. This can have several effects on radio systems. The reflection process is determined by the reflection coefficient. As we know, both amplitude and phase changes take place at the point of reflection since the coefficient is in general complex. Thus, if $\boldsymbol{E}_i$and $\boldsymbol{E}_r$ are determined as the incident and reflected fields before and after the reflection point, we can write [8]

$$\boldsymbol{E}_r = \rho \boldsymbol{E}_i \ , \tag{4}$$

where ρ indicates the complex reflection coefficient. The reflection coefficient depends on the electrical properties of the two media, the angle of incidence, the frequency, and polarization of the incident signal. In the case of p-polarization, the electric field is parallel to the normal of the surface; in the case of s-polarization, the electric field is perpendicular. These refer to the relationship of the incident electric vectors with the plane containing the incident and reflected waves. The following electrical

properties must be known for the two media to calculate the complex reflection coefficient at a plane boundary between them.

Permittivity is defined by

$$\varepsilon = \varepsilon_0 \varepsilon_r \,, \tag{5}$$

where $\varepsilon_0 = 8.854.10^{-12}$ Fm^{-1} is the permittivity of vacuum and ε_r is the relative permittivity.

Permeability is defined by

$$\mu = \mu_0 \mu_r \,, \tag{6}$$

where $\mu_0 = 4\,\pi \cdot 10^{-7}$ Hm^{-1} is the permeability of vacuum and μ_r is the relative permeability.

Two important characteristics of radio waves are derived from these quantities.
The ratio of the electric and magnetic field is called the wave impedance

$$\eta = \sqrt{(\mu/\varepsilon)} \,. \tag{7}$$

The wave impedance of vacuum, $\eta_0 = \sqrt{(\mu_0/\varepsilon_0)} \approx 377\Omega$ and the wave velocity is denoted as

$$c = \sqrt{1/(\mu\varepsilon)} \,. \tag{8}$$

The wave velocity in vacuum, $c_0 = \sqrt{1/(\mu_0\varepsilon_0)} = 2.998 \cdot 10^8$ ms^{-1}

2.2.2. Refraction

Refraction means the change in direction and velocity of the electric field when it passes from one medium into another. Consider the case, the wave passes air to glass and travels through the glass. Now by approaching the surface at an angle consider the wavefront, we can observe the fact that the wavefront bends as it passes from air to glass. The bending occurs because the wavefront does not travel as far in one cycle in the glass as it does in the air. The wavefront into the glass travels a smaller distance in glass than it does in air, causing it to bend in the middle. Thus, the wave, which is perpendicular to the wavefront, also bends. The incidence angle and the indices of refraction of glass and air is responsible for the amount of bending, which determines the change in speed.

From Figure 1, it is possible to explain the Snell's law for angle of refraction or the law of refraction [9]

For $\mu_1 = \mu_2$ it can be written

$$\frac{sin\theta_2}{sin\theta_1} = \sqrt{\frac{\varepsilon_{r_2}}{\varepsilon_{r_1}}}, \tag{9}$$

where medium 1 is a vacuum (or air), Snell's law is often quoted in terms of the refractive index of the other material. Refractive index n is given by:

$$n = c/v, \tag{10}$$

where c and v are the velocities in vacuum and the material, respectively. Thus

$$n = \sqrt{\varepsilon_r}. \tag{11}$$

This is the law which relates the angle of incidence and the angle of transmitted wave at the interface of two different media. The law is applicable for all materials. The case of refraction is more complicated than reflection and thus understanding of Snell's law is compulsory. Now, from Figure 1 calculating the unknown index is easier with a known refractive index by measuring angles and applying Snell's law.

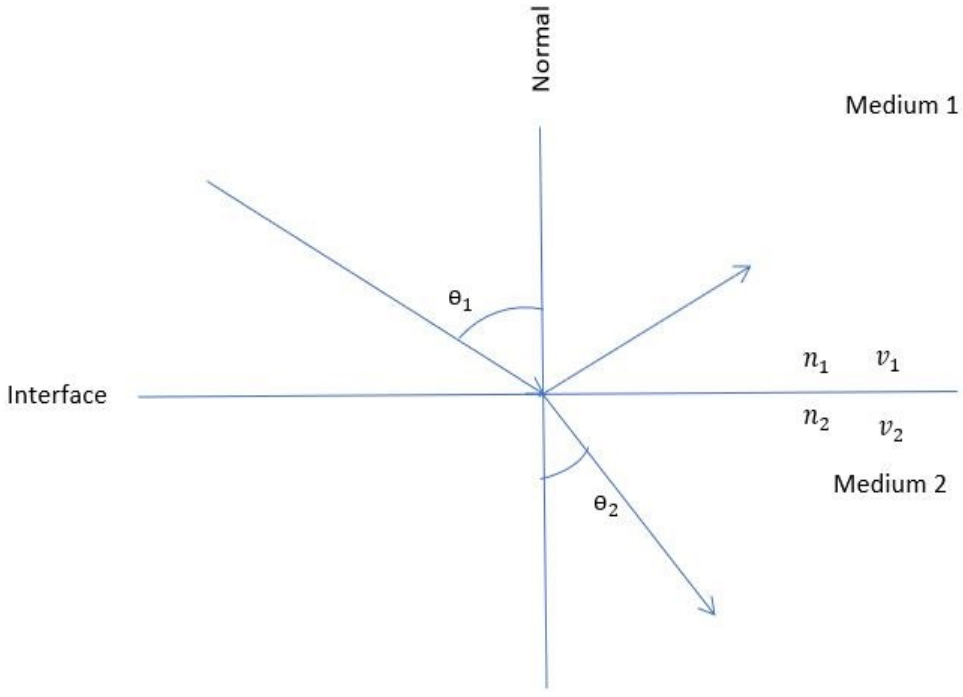

Figure 1. Reflection and refraction between two media

2.2.3. Diffraction

Diffraction is such a characteristic that occurs when a wave meets with an obstacle or an opening. The diffracting objects are crucially becoming a secondary source of the propagating wave. Diffraction introduced a change in the direction of waves as they are passing by an opening or around a barrier in their way of propagation. The amount of diffraction is larger if the wavelength of the wave is large. Diffraction is possible when the gap size is about the same as the wavelength of the wave. So that the minimum intensity occurs at an angle θ_{min} given by $wsin\theta_{min} = \lambda$, where *w* denoted as the width of the opening, θ_{min} is known as the angle of incidence at which the minimum intensity occurs, and λ is the wavelength of the electromagnetic wave [10].

The intensity can be measured by using the Fraunhofer diffraction equation as

$$I(\theta) = I_0 sink^2(\frac{w\pi}{\lambda} sin\theta), \tag{12}$$

Where *I(θ)* is the intensity at a given angle, I_0 is the original intensity, and the unnormalized *sink* function above is given $sink(x) = \frac{sinx}{x}$ if $x \neq 0$ and *sink*(0)=1.

2.2.4. Absorption

An amount of electric charge is received by a particle when the electromagnetic wave is outcasted on it and resulting the transference of radiation energy and momentum [11]. Energy is absorbed from the wave and some amount of energy is reflected. Absorbing energy from electromagnetic wave is possible, consider as the examples is a black surface. It becomes hot from absorbing waves and little of them are reflected making the surface appear black. If the surface is painted with a white covering, it will reflect more of the waves and absorb less. Thus, a white surface will be cooler.

2.2.5. Polarization

Radio wave polarization is determined by the electric field traces out with time at a fixed observation point. A wave is linearly polarized when the polarization plane of an antenna collapses to a line and has an infinite axial ratio. Whereas a circularly polarized antenna means the plane rotates in a circle and complete one complete revolution during each period of the wave. If the plane of propagation rotates clockwise, it defined as right-hand-circular (RHC) and if it is counter-clockwise, it is called left-hand-circular (LHC) [12]. A vertically polarized (linear) antenna is one whose electric field is perpendicular to the plane surface. If the electric field parallels to the plane surface, this known as the horizontally polarized (linear) antenna. For a circularly polarized wave, the energy is radiated in both horizontal and vertical planes. The difference between the maximum and the minimum peaks as the antenna is rotated through all angles, known as the axial ratio or ellipticity and is usually measured in decibels (dB). If the axial ratio is equal to 0 dB then the antenna is ideally circular polarized but in the real world, we consider a circularly polarized antenna which having axial ration near 0 dB. We can say an antenna is elliptically polarized if the scale of the axial ratio is

greater than 1-2 dB. To earn the best efficiency, we must use an antenna by maintaining the same polarization on both ends of a communications path. The electric field can oscillate in any direction normal to the direction of wave propagation (which is parallel to the k vector). Presume that an electromagnetic wave in a plane is propagating in the z-direction. It follows that the electric field can oscillate in the x-y plane. The polarization of the wave is determined by the actual oscillation direction of the electric field. An electromagnetic wave in a vacuum having an angular frequency (ω) that is polarized in the direction of e_x has the associated electric field [13]

$$E = E_0 \cos(\omega t - kz) e_x \,, \tag{13}$$

where $\omega = kc$. Similarly, a wave that polarized towards e_y direction has the electric field [13]

$$E = E_0 \cos(\omega t - kz) e_y \,. \tag{14}$$

The electric field vector of these two waves are oscillating to a line which means they are linearly polarized. Now, by combining this linearly polarized waves with different (x-direction, y-direction) directions can possible to obtain a circularly polarized wave [13]

$$E = E_0 \cos(\omega t - kz)\, e_x + E_0 \cos(\omega t - kz)\, e_y \,. \tag{15}$$

This term arises from the fact that the tip of the electric field vector traces out a circle in the plane perpendicular to the direction of wave propagation. To be more exact, the previous wave is a *right-hand* circularly polarized wave, since if the thumb of the right-hand points in the direction of wave propagation then the electric field vector rotates in the same pattern as the fingers of this hand and its vice-versa for a left-hand circularly polarized wave [13]

$$E = E_0 \cos(\omega t - kz)\, e_x - E_0 \cos(\omega t - kz)\, e_y \,. \tag{16}$$

Finally, if the x and y components of the electric field in the previous two expressions have different (non-zero) amplitudes then we obtain right-hand and left-hand elliptically polarized waves.

2.2.6. Scattering

Scattering is depending upon the wavelength and particle size of the electromagnetic waves. During propagation, electromagnetic waves possibly can interact with particles or discontinuities, and locally outface the local electron distribution. This variation provides periodic charge separation within the particle causing oscillation of the induced local dipole moment acting as a source of electromagnetic radiation thus causing scattering. Most of the scattered waves oscillate at the same frequency as the incident wave, and are termed elastic scattering. Interaction with the incident beam may also responsible for absorption. Generally, electromagnetic waves scattered by particles can be explained by two theoretical frameworks: Rayleigh scattering that may apply to small, dielectric, non-absorbing spherical particles, and Mie scattering that provides a general solution to scattering independent of particle size. Mie scattering theory gives a generalized approach which has no particle size limitations and converges to the limit of geometric optics for large particle sizes. The size of the particle and the wavelength of the illuminating radiation is the base of Rayleigh scattering [14]. The intensity is increased rapidly with the ratio of particle size to wavelength increases in case of Rayleigh scattered radiation. If the particle radius is much smaller than the wavelength of incidence wave, then the scattering is called "Rayleigh scattering".

The incident E-field induces a dipole moment which is time-varying in the sphere. This dipole radiates like a Hertzian dipole, and this radiation is the scattered radiation. Consider the z-directed E-field phasor for the incident plane wave at the location of the particle is: $\hat{E}(\acute{r}=0) = Ei$, the dipole moment phasor P induced in the sphere is therefore [15]:

$$P = 4\pi\varepsilon_0 a^3 \left(\frac{\varepsilon_1-\varepsilon_0}{\varepsilon_1+2\varepsilon_0}\right) E_i \ . \tag{17}$$

Total scattered power P_s from a dielectric sphere is

$$P_s = \frac{4\pi}{3\eta_0} k^4 a^6 \left(\frac{\varepsilon_1-\varepsilon_0}{\varepsilon_1+2\varepsilon_0}\right)^2 |E_i| \ , \tag{18}$$

and the scattering cross section of the scatterer is expressed as

$$\sigma_s = \frac{8\pi}{3} k^4 a^6 \left(\frac{\varepsilon_1-\varepsilon_0}{\varepsilon_1+2\varepsilon_0}\right)^2 , \tag{19}$$

where, $\frac{(|Ei(r)|^2}{2\eta 0}$ the incident power per unit area. σ_s is the ratio of the total scattered power to the power per unit area of the incident wave at the scattering location.

2.2.7. Path loss

Path loss means the reduction of power density or signal attenuation during the path of signal propagation. This is the most common component used to analysis the link budget. Consider P_T as transmitted power radiated from an isotropic antenna. This antenna refers as a point source who can radiates power uniformly in all directions. Assume that the point source is placed in a position such as the antenna sphere with radius d is centered on it.

If the free-space transmission is assumed the radiated power density will be uniform at all points on the sphere's surface. The total transmitted power P_T will pass outward through the sphere's surface. Then the radially directed power density can be expressed as

$$P_D = P_T/4\pi d^2 \ . \tag{20}$$

If the effective area A_R of receiving antenna is located on the surface of the sphere, the power density times with area of the antenna should be equal to the total receive power P_R. This is expressed as [16]

$$P_R = P_T(A_R/4\pi d^2) \ , \tag{21}$$

the effective area A_T of transmitting antenna concentrates its radiation within a small solid angle or beam thus, an on-axis transmitting antenna gain is achieved, with respect to an isotropic radiator, of

$$g_T = 4\pi \, A_T/\lambda^2 \ . \tag{22}$$

Let's use this antenna in place of the familiar isotropic radiator. Then the equation for receive power

$$P_R = P_T(4\pi \, A_T/\lambda^2) \cdot A_R/4\pi d^2)$$

$$\Rightarrow P_R = P_T(4\pi \, A_T/\lambda^2) \cdot P_T(4\pi \, A_R/\lambda^2).(\lambda/4\pi d)^2$$

$$\Rightarrow P_R = P_T(g_T) \cdot \ (g_R) \cdot (\lambda/4\pi d)^2 \ . \tag{23}$$

Thus, in decibels, the ratio of P_T to P_R is

$$10\log(P_T/P_R) = 20\log(4\pi \, d/\lambda) - 10\log(g_T) - 10\log(g_R) \ , \tag{24}$$

where the distance and frequency dependent term in the equation define the free space path loss. So, the free space path loss in term of frequency can be given by

$$FSPL = 20\log(\frac{4\pi df}{c}) . \quad (25)$$

2.2.8. Multipath fading

A random process by which the variation of attenuation with various variables of a signal is considered as fading. Fading mechanisms involved with refraction, reflection, diffraction, scattering and attenuation of radio waves. Fading can be multipath induced due to multipath propagation or can be shadow fading by the effect of shadowing. Generally, frequency diversity is considered as one of the best techniques for reducing multipath fading because multipath fading is usually frequency selective.

3. COMPLEX DIELECTRIC CONSTANT

Dielectric materials have an important role in electronic device. Dielectric materials are used for high frequency electronic circuits and the dielectric properties of the material drive the circuit operation. A dielectric material will be polarized under an electric field and the dielectric properties carries valuable information regarding the storage and dissipation of electric and magnetic fields in materials [17] . An electric dipole is the effect of two equal charges of opposite polarity separated from each other by a small distance. The electric field is produced by the electric dipoles in the dielectric materials. The electric field is uniform and at the edges there is a fringing of the electric flux. The electric flux density is also uniform in that region. The dielectric constant ε_r is measured as a ratio of electric flux density to electric field intensity.

3.1. Definition of dielectric constant

If a capacitor with capacitance C and a voltage V is applied, then the charge Q is directly proportional to the applied voltage and capacitance. The capacitance depends on the permittivity ε, as well as the area A of the capacitor and the distance of separation between the two conductive plates. Permittivity and capacitance are mathematically related as [18]

$$C = \varepsilon \frac{A}{d} . \tag{26}$$

The dielectric constant of a material is the ratio of its permittivity to the permittivity of vacuum. So that it can be written as

$$\varepsilon_r = \frac{\varepsilon}{\varepsilon_0} . \tag{27}$$

The dielectric constant is also known as the relative permittivity of the material. Since the dielectric constant is just a ratio of two similar quantities, it is dimensionless.

3.2. Effect of dielectric constant

Radio waves travel in different parts of a medium. These different parts of a medium consist different dielectric constant. Dielectric constant can be used to recognize the interaction between electromagnetic wave and material. Zero conductivity is expected by a perfect dielectric, but most real-world materials have both a dielectric constant and a nonzero conductivity. The dielectric becomes more lossy when the conductivity of the dielectric material is increased. In case of non-ideal materials that effects on electromagnetic wave, the permittivity works as a function of the conductivity, and the frequency of the wave. The propagation speed is depended upon the permittivity. Dielectric properties are related to the other properties of material or environment, e.g. variation of temperature can effect on dielectric properties. The increase of temperature is responsible for decrease in permittivity and drops in dielectric constant [19].

3.3. Interaction in boundary of two medium

On material boundaries to describe the impact of electromagnetic waves, it is crucial to determine the polarization angle of the plane of incidence. Consider the material as non-magnetic. From Figure 1 it can be observed that an electromagnetic wave incident in a dielectric boundary, when travelling from one medium to another, some of it is reflected and some transmitted. Snell's law gives the relationship. It can be obtained from equations 13 and 14 and can written as

$$n_1 sin\theta_1 = n_2 sin\theta_2 \,, \tag{28}$$

and

$$\sqrt{\varepsilon_1} sin\theta_1 = \sqrt{\varepsilon_2} sin\theta_2 \,. \tag{29}$$

There could be possible, an angle is such that the total incidence wave is transmitted means of no reflection. The incidence angle where the incidence wave is totally transmitted known as Brewster angle or the angle of polarization. It depends on the dielectric properties and given by [20]

$$\theta_b = tan^{-1}\left(\sqrt{\frac{\varepsilon_2}{\varepsilon_1}}\right) . \tag{30}$$

Brewster angle is measured by the incident angle for which the reflected wave is polarized perpendicular to the incidence plane for any polarization of the incident wave [21]. This leads the case of parallel mode the reflection coefficient is zero or totally transmitted. The Brewster angle relates to the dielectric properties of the material. So, it is possible to measure the dielectric constant of the material if the Brewster angle is known.

4. CHANNEL MODELLING

Channel modelling in wireless communication has always been an important topic. It has gained rapid development within a few eras due to the development and advancement of wireless technologies. The aim of future wireless services to provide future generation mobile communication systems to be used in low- mobility environments with limited temporal or multipath diversity.

4.1. Tapped delay line model

A system model with at least one "tap" creates a delay line is known as the tapped delay line. It exacts the signal output from the delay line, optionally scales it and linearly sums with other taps to form an output. It can efficiently simulate multiple echoes by unchanging the source signal thus the popularity of using a tapped delay line model is increased [22]. An example can be shown by the below Figure 2 for explaining the tapped delay line. The total length of the delay line is A_2 samples and the output of the model is the linear combination of the input signal *x(n)* the tapped delay line output (x-A_2) and the tap signal x(n-A_1*)*.

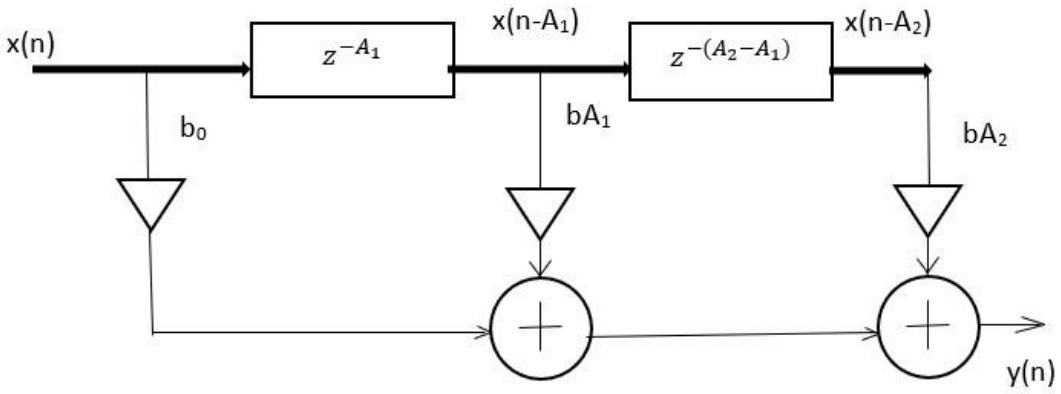

Figure 2. Tapped delay line model [22].

The difference of the TDL of Figure 2 is, by inspection

$$y(n) = b_0 x(n) + b_{A_1} x(n - A_1) + b_{A_2} x(n - A_2)\ , \tag{31}$$

where the *y*(*n*) is the output of the model and the corresponding transfer function is

$$H(z) = b_0 + b_{A_1} z^{-A_1} + b_{A_2} z^{-A_2}\ . \tag{32}$$

This transfer function provides the outputs of each possible input. In some application transpose of the above the system model is essential. This transpose TDL can be obtained by the formal transportation of above system diagram. A TDL is also suitable

for parallel processing. TDL is the based concept of finite impulse response (FIR) filter. A FIR filter is based on a feed-forward equation. Feed-forward means that there is no feedback of past or future outputs to form the present output.

4.2. Indoor channel models

For RF communications such as wireless LANs, wireless keyboard or mouse, cordless phones indoor propagation of electromagnetic waves is the heart of the communications. The environment of indoor is pretty much different than the environment of outdoor. It is different due to many facts like building structure or construction materials. The environment also can be changed by the indoor activities like the movement of people, closing doors etc. thus, an indoor environment using a deterministic model is not suitable. In outdoor environment operating distance is larger but in the indoor environment its smaller near about few meters or sometimes it can be few centimeters. So, interference can occur, and it's become very unfriendly. By computing the signal-to- interference ratio at the receiver, the effect of various interference can be estimated.

The principal characteristics of an indoor RF propagation environment that differentiate it from an outdoor environment are that the multipath is usually severe, and the characteristics of the environment can change drastically over a very short time or distance [23]. The ranges involved tend to be rather short, on the order of 100 m or less. Walls, doors, furniture, and people can cause significant signal loss. Indoor path loss can change dramatically with either time or position, because of the amount of multipath present and the movement of people, equipment, and/or doors. When considering an indoor propagation channel, it is apparent that in many cases there is no direct line of sight between the transmitter and the receiver. In such cases, propagation depends upon some properties like reflection, diffraction and scattering. Fading can affect also in degrade a signal. Delay and Doppler spread are usually less significant in an indoor environment as compared to outdoor environments. In addition, the wave may experience depolarization, result in polarization loss at the receiver. There are two general types of propagation modelling: site-specific and site general. Site-specific modelling requires detailed information on building layout, furniture, and transceiver locations. It is performed using raytracing methods in a CAD program [24]. For large-scale static environments, this approach may be viable. For most environments, limited knowledge of building layouts and materials and the environment itself can turn into moving furniture or doors. This is the reason why the site-specific technique is not commonly employed. Site-general models are generally used because it provides gross statistical prediction of path loss for link design and are useful tools for performing initial design and layout of indoor wireless systems [25].

4.3. MIMO channel models

Multiple Input Multiple Output (MIMO) system is the concept of providing higher throughputs within a given bandwidth. The connection between the transmitter (TX) and receiver (RX) is described by the MIMO channel. Figure 3 illustrates a 2×2 MIMO system. It shows that 2 antennas are used in TX and 2 for RX. The MIMO system is demonstrated with the channel matrix $\boldsymbol{H}$ and scattering medium is present around it.

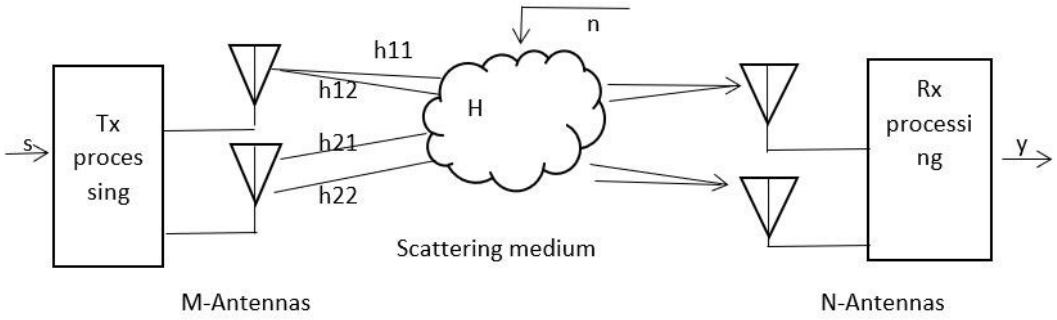

Figure 3. 2×2 MIMO system [26].

For the above M and N indicates number of TX and RX antennas respectively. The input and output relationship can be expressed as [26]

$$y(t) = \boldsymbol{H}(t) * s(t) + n(t) \,, \tag{33}$$

where $y(t)$ is the received signal, $\boldsymbol{H}(t)$ is an M×N channel impulse response matrix, $s(t)$ is the transmitted signal, $n(t)$ is additive white Gaussian noise (AWGN), and $*$ denotes convolution. By simplifying the above input-output relationship the equation becomes

$$y = \boldsymbol{H}s + n \,. \tag{34}$$

Matrix $\boldsymbol{H}$ is effective for describing the propagation channel between all transmit and receive antennas. Now considering the noise the representation of $\boldsymbol{H}$ should be expressed as

$$\boldsymbol{H}(\tau) = \sum_{i=1}^{L} \boldsymbol{H}_i \delta(\tau - \tau_i) \,, \tag{35}$$

where L is the number of taps of the channel model. The MIMO channel models is divided into the wideband models and the narrowband models depending on the bandwidth of the system. Wideband propagation channels are treated as frequency selective, meaning that different frequency sub-channels have different channel response. In case of narrowband models, the channels have frequency non-selective fading, and thus the channel response is same over the total system bandwidth [26].

5. MEASUREMENT TECHNIQUES

This chapter is first describing various channel measurement techniques, and then focuses on the measurement techniques for dielectric characteristics. Last part of this chapter presents different measurement scenarios are performed regarding this project work.

5.1. Channel measurement methods

Wideband multiantenna multiuser systems are more and more popular. Important features of the radio channel for example are the channel's frequency selectivity, directivity, polarimetric properties, and their relation to channels of the other users are becoming obvious. After completing the measurements one can have a bundle of data, and these are analyzed to get desired results. Due to a bulk number of measurement campaigns, different measurement methods are addressed such as distributed cooperative systems, the polarimetric channel, vehicular channels under high mobility, ultra-wideband channel sounding, and millimeter and submillimeter-wave systems. The first part of this chapter gives an overview of ultra-wideband channel sounding, and millimeter and submillimeter-wave systems.

5.1.1. Ultra-wideband channel sounding

Ultrawide frequency bands are handling by the ultra-wideband (UWB) channel sounding. Equipment that can deal with UWB is needed. A test instrument called vector network analyzer (VNA) is capable to cover these frequency bands, and it is used commonly in many labs. The key advantage of VNA-based measurement is a large and flexible dynamic range of the measurement bands. The major disadvantages are its requirement of RF cables to connect the TX and RX antennas, and due to the sequential scanning of frequency points, the measurement speed is time-consuming. With an optional time, domain transformation capability, channel sounding can be done also in the time domain.

Time-domain channel sounding uses commonly two methods. One method is the transmission of short pulses that results directly at the receiver as a channel impulse response. The bandwidth of the transmitted pulse is determined the time resolution. However, it is difficult to generate pulses with a short rise time, and the pulse energy is decreased due to increasing bandwidth which results in very low power.

PN sequence as a sounding signal can be defined as the second method. It transmits digital symbols instead of isolated pulses, and by this continuous transmission it increases the average power of the transmitted signal. The frequency-domain channel sounding can be defined by M-sequence channel sounding. In that case, the channel sounder is based on maximum length binary sequence (MBLS). The channel sounder generates an MBLS by using the shift register, and the obtained baseband signal is up converted to cover the desired frequency band. In M-sequence channel sounding, calibration is the key step. Finally, the system response is taken from the transmit and receive ports. The accuracy of measurement is verified by comparing a standard measurement done with a VNA.

5.1.2. Millimeter and submillimeter-wave systems

Millimeter waves (mmW) and submillimeter waves (sub-mmW) can provide promising solutions for broadband data rates in short-range communications. It has become a challenge to transmit of multi-Gbit/s data with such frequencies. Successive mmW/sub-mmW solutions can reduce the use of wires in between a local network. The environment of short-range communication differs due to many things such as a higher density of users, diffraction from human bodies, metal cabins, etc. So, during channel modelling, a designer must consider all the possible obstacles and thus channel characterization of different scenarios and antenna patterns are important.
UWB channel sounder can be a solution. This channel sounder should be based on M-sequence UWB channel sounding. At UWB stage, using of multiple modules can be able to support distributed MIMO. The system should have a common chain to obtain I and Q signals for calibration purposes. Thus, a serial I/Q concept can be implemented with 90° local oscillator (LO) phase sifting. Frequency modulation continuous wave (FMCW) techniques can be another sounder implementation. In this case, a continuous wave signal is repeated excite the channel and the phase noise can be predicted [27].

5.2. Measurement techniques for dielectric properties

There are many measurement methods to find the dielectric properties of materials such as, coaxial probe method, transmission/reflection line method, free space method, resonant cavity method, parallel plate method. The open ended co-axial probe method is assuming only the TEM or TE mode is propagating. In this method, for measuring the reflection coefficient the probe is immersed into the liquids, and the permittivity is determined. Dielectric probe is used to measure the complex dielectric constant of the material. The flat face of a material is brought under touch of the probe, the electromagnetic field of the probe is penetrated into the material, and the reflected signal (S_{11}) is measured [28]. This is an easy technique, but the accuracy is very poor.
The transmission/reflection line method is the most popular one for measuring dielectric properties. It is assumed that the fundamental waveguide mode is to propagate. A dielectric material is placed inside the transmission line and an electromagnetic wave is directed towards it. A VNA is used for measuring complex two port scattering parameters [29].
Free space method allows materials under test (MUT) for different environments such as high temperature, wide band frequencies. Free space method need two antennas connected to a VNA and between these two antennas a sample holder is needed where the material is to be placed [30].The VNA is then responsible for measuring the S-parameters. The accuracy is achieved better on high time domain analysis. Resonant cavity method provides high accuracy. This typically consist of metallic cavity that resonate at specific frequencies. A piece of MUT is placed into the cavity that affects the resonant frequency (f) and quality factor (Q) of the cavity [28]. The complex permittivity of the material is calculated at a single frequency by using these parameters. A typical network analyzer may consist of a measurement system with a resonant cavity fixture and software to make the calculations. A parallel plate capacitor used as a sample holder in parallel plate method. Impedance analyzer is needed for this method. The measured capacitance and dissipation is used to calculate the dielectric properties [31].

5.3. VNA based measurement system

Vector network analyzer (VNA) is one of the best instruments in radio engineering and applications. The measurement results are essential in the most modern application such as device characterization or antenna tests etc. The ports of the VNA allow real-life circuit-type parameters from devices under test (DUT). The VNA characterizes high-frequency passive and active devices in their linear mode of operation by measuring their network parameters, called S-parameters, as a function of frequency [32]. Modern VNAs are updated and extended in hardware that they can also measure noise parameters and nonlinear characteristics. Therefore, the VNA can perform multiple measurements by a single setup. The VNA is popular for its accuracy and high dynamic range. It supports probing and adapter removal. The instrument provides step and impulse response information. Dealing with VNA is very easy or can say it is a user-friendly device. The data format can be changed according to demand. Working with frequency parameters are common because the analysis is done usually in the frequency domain. The transition from a frequency domain to time domain can be done by the inverse Fourier transform either directly in VNA or in a post-process using an analysis software. The measurement frequency range and the number of selected frequency points over the given frequency band are input options for a VNA measurement. Although the VNA has too many advantages, it also has some drawbacks such as the long sweep time, limited measurement cable length, instrument costs etc.

5.3.1. Proposed measurement system

Figure 4 and 5 show the block diagram and the practical view of the measurement system in different scenarios. In Figure 4, the LOS measurement system is shown where antennas are faced to LOS direction for a reference measurement before they are tilted to look at the reflecting plywood sample. Hence, when monitoring the signal in time domain it shows the reflection impact also. In case of Figure 5, a sheet of absorber material is placed between the two antennas to attenuate the LOS signal. Here, MATLAB is used as centralized control software to control the devices and store the measurement data. General purpose interface bus (GPIB) was utilized to communicate with the VNA. The used analyzer was 8720ES [33]. It should be considered that the antenna was not moving when VNA is performing the sweep. In this work, many other different scenarios have been performed, and the collected data are provided in a later chapter.

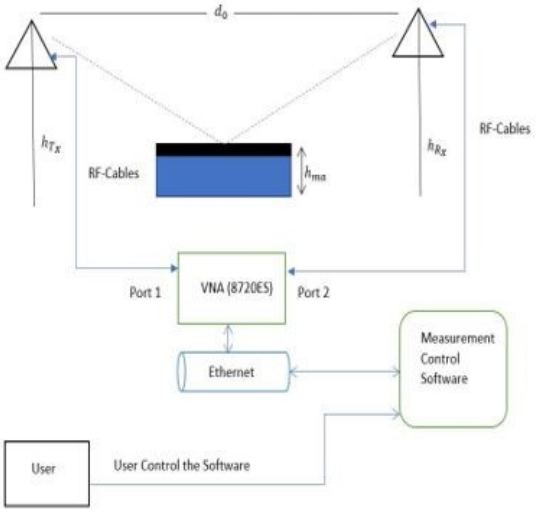

Block Diagram of LOS measurement system

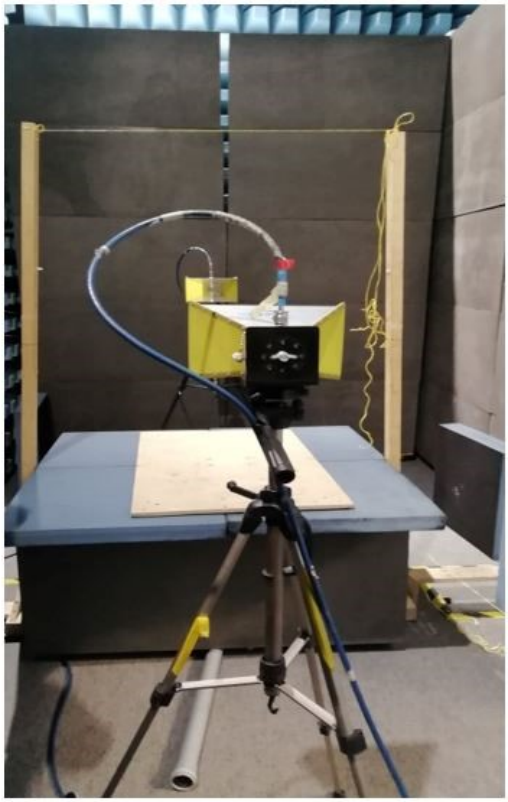

Practical View of LOS measurement system

Figure 4. LOS reference measurement.

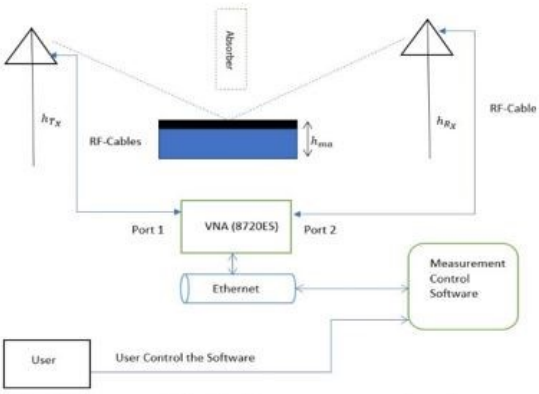

Block Diagram of Reflection measurement system

Practical View of Reflection measurement system

Figure 5. Reflection measurement.

5.3.2. Measurement setup

The key concept is to find the dielectric constant of different dielectric materials. Free space method for measurement is used in an anechoic chamber at university of Oulu. A VNA (8720ES), two antennas (R & S HF906) as TX and RX, and RF cables are used for this setup. The basic setup data specifications are described in Table 1.

Table 1: Basic setup data for measurements

Antenna gain	10.5 dB
Number of points	1601
Frequency ranges	1-9.5 GHz, 9.5-18 GHz
Cable length	16 meters
Distance from TX to RX	2.94 meters

The 2-port VNA system is used as a source to collect the data and to display the responses in terms of S-parameters. GPIB interface is used to connect the VNA with a laptop and to collect and store the data for later analysis with MATLAB.

5.3.3. Antennas

An antenna is the basic component which provides the interconnecting links between transmitter and receiver via free space. In this experiment, the role of antennas is very crucial. Here, double-ridged waveguide horn (R & S HF906) antennas [34] are used. Their key features include:

- broadband compact transmitting and receiving antenna,
- frequency range 1-18 GHz,
- gain 7-14 dBi,

Positioning, tilt angles, polarization attitude, and the heights of the antennas were varied to collect the data in different scenarios. Polarization of antenna is defined by the polarization of wave transmitted by the antenna. The antennas are not ideal radiative components, and it makes sense that not all power fed into it is necessarily radiated. Antenna matching is not measured for this setup. Instead, the reflected signal strength is compared to the direct LOS reference signal, and the path distance difference is compensated from the result.

5.3.4. Scattering parameters

Scattering parameters are needed to find the relationship between the incident, reflected and transmitted waves. The Scattering parameters (S-parameters) are presented as a function of frequency in a matrix structure. This is basically a mathematical structure that specify the propagation of a RF-signal in a multiport network. S-parameters of a network is the basic of finding the properties of an electrical network such as impedance, attenuation, dielectric properties, VSWR. S-parameters are given complex numbers, having magnitude and phase of the incident wave with real and imaginary parts [35]. In this case, VNA is used for collecting data from parameter S_{21}, which yields the impulse response related to the radio channel. The S_{21} is analysed for getting the ρ.

5.3.5. Calibration

The instrument can be responsible for several errors in measurement. Environmental effect can change the properties of the instrument. Therefore, the VNA should calibrated before measurement in such a way that all effects due to the VNA are removed. RF cables and adapters are used as the transmission line between the VNA ports and the antennas. Calibration removes the effect of these components. The calibration can

be verified by connecting them in a direct loop, and checking the response. Another issue is the component temperature drift that can lead to errors. To minimize the errors due to temperature variance, VNA needs to be turned on for a certain time before taking measurement. Some other noises from VNA and environment can take places during measurement, but generally their effect can be neglected. There are several calibration methods, but only a few of them supports the use of calibration kit for a VNA.

6. RESULTS AND ANALYSIS

6.1. Verification of the measurement setup

The verification of measurement system is very necessary. If the measurement system works properly, one may go for the real experiment. For verification of measurements, a possible stable LOS-propagation environment is created. Later, this measurement is used as a reference measurement for the measurements. The measurement system was assembled in the anechoic chamber by building a small compartment using absorber blocks. However, the metal floor of the chamber was not covered by absorbers. Instead, the material under test was elevated on top of an absorber block, and the reflection from the MUT was separated in time domain. Figure 6 shows the LOS reference path delay and the respective power. This data can be utilized as LOS reference for measurements carried out on days Oct 16 and Oct17, irrespective of the polarization scenario.

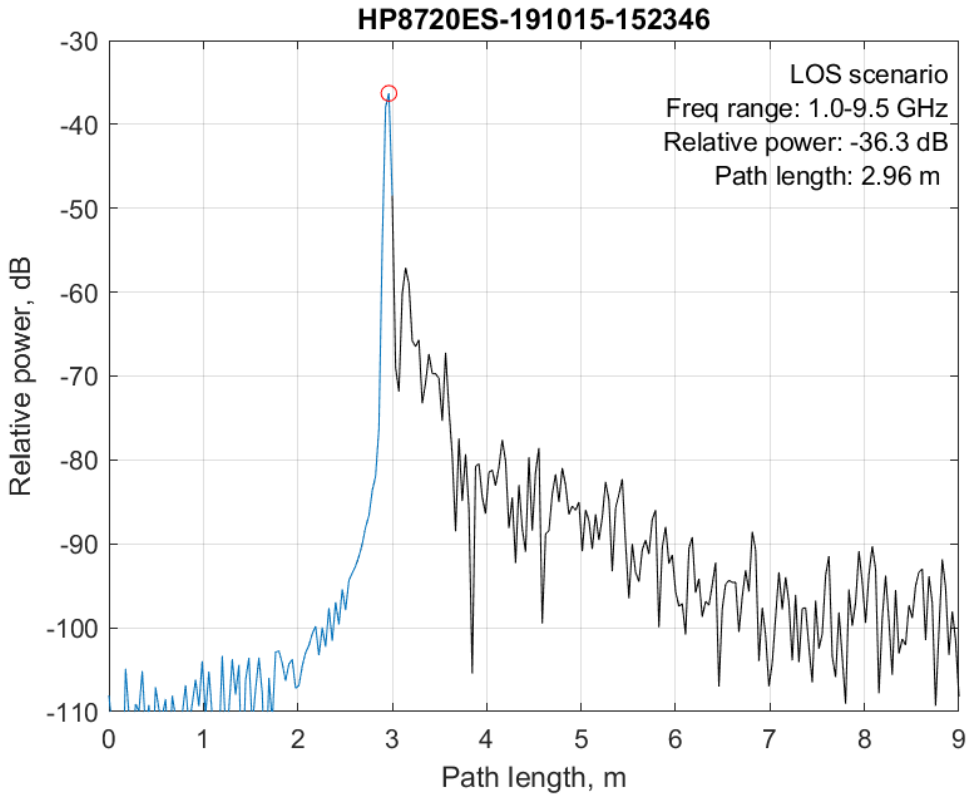

Figure 6: Measured LOS impulse response.

6.2. Sample measurement of the selected frequency ranges

The measurement is done in two successive frequency bands. The lower band is from 1.0 to 9.5 GHz and the upper one is from 9.5 to 18 GHz. The experiment is done in different scenarios with 1601-point frequencies over each band. This number of points allows the data to be analyzed in narrower sub-bands if needed, still yielding a non-

aliased impulse response. The measurements are taken for s-polarization and p-polarization. The aim is to find the relative permittivity via Brewster angle by studying the reflection coefficient of a p-polarized signal. A part of measurement scenarios is showed in Figure 4 and Figure 5.

6.3. Analysis of the measurement results

The collected data is extracted and analyzed utilizing a MATLAB program. As mentioned, the recorded data is the S_{21} parameter measured over the radio channel. Reflection coefficient is calculated from the time domain data as a ratio of the reflected path power to the power of the LOS path. The angle of incidence is also calculated form the TX and RX coordinate data.

Now, for measuring the relative permittivity, the equations are

s-polarization/perpendicular polarization:

$$\rho = \frac{cos\theta_i - \sqrt{\varepsilon_r - sin^2\theta_i}}{cos\theta_i + \sqrt{\varepsilon_r - sin^2\theta_i}}, \tag{36}$$

p-polarization/parallel polarization:

$$\rho = \frac{\varepsilon_r cos\theta_i - \sqrt{\varepsilon_r - sin^2\theta_i}}{\varepsilon_r cos\theta_i + \sqrt{\varepsilon_r - sin^2\theta_i}}. \tag{37}$$

Two different frequency ranges (1-9.5) GHz and (9.5-18) GHz are used for this experiment. Figures 7 and 8 show the LOS reference signal used for calculating the reflection coefficient on Oct 29.

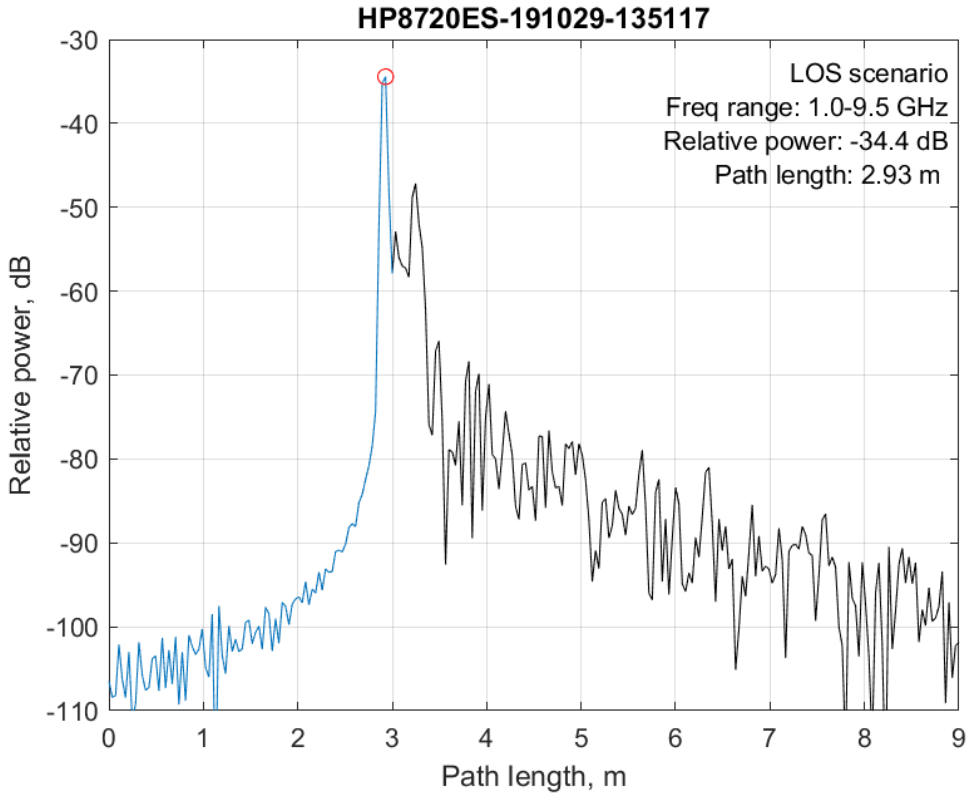

Figure 7: Reference signal at 1-9.5 GHz frequency range.

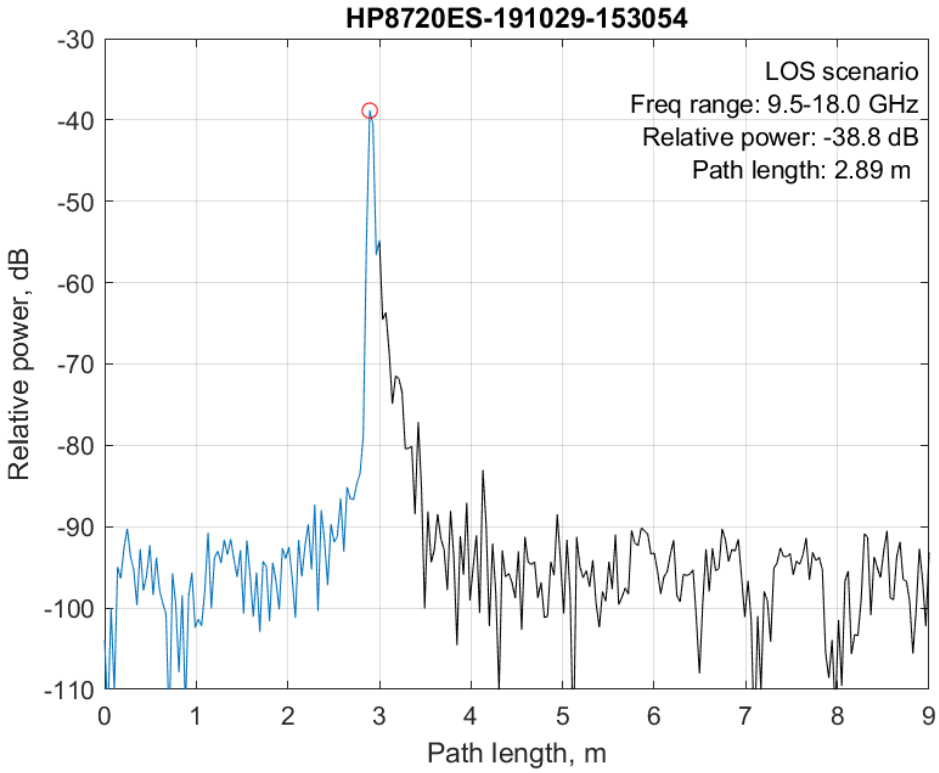

Figure 8: Reference signal at 9.5-18 GHz frequency range.

The sample data for both p-polarization and s-polarization at frequency ranges 1.0-9.5 GHz and 9.5-18 GHz are plotted in Figures 9, 10, 11 and 12 respectively. The incident angles are about the same, and the power level difference is 4.5 dB in favor for the s-polarization. Notice that the antennas were tilted to face directly the material sample. The LOS path is generated by the side lobes of the antennas during the reflection measurements is ignored in the analysis phase. Only the pure LOS paths presented in Figures from 6 to 8 are used as references.

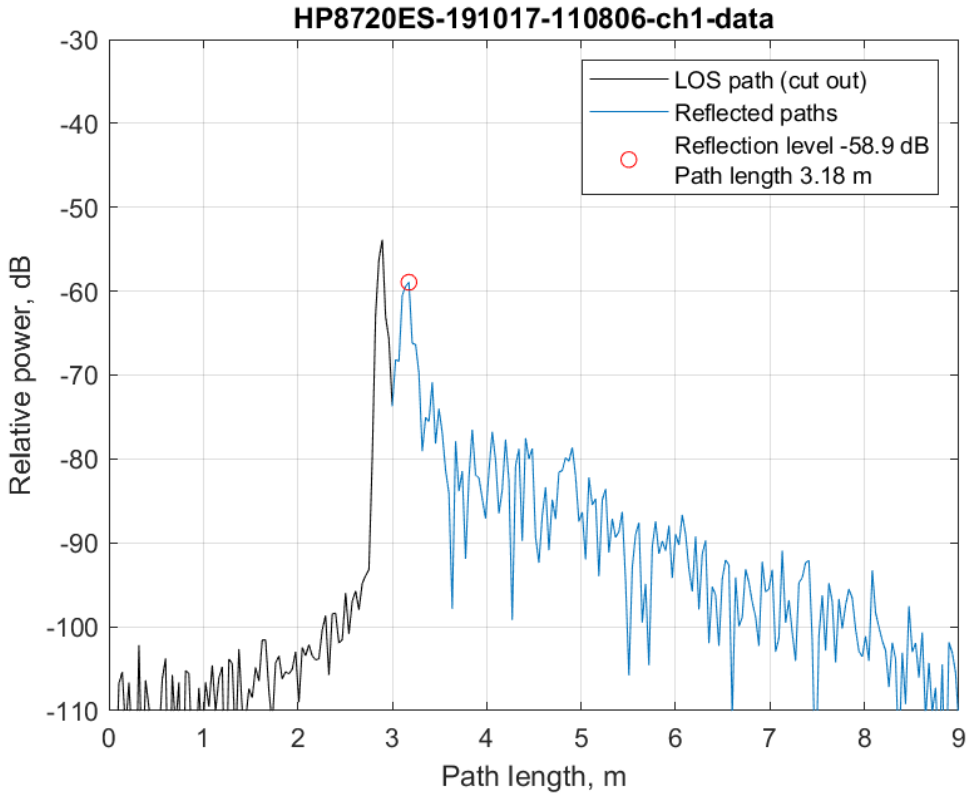

Figure 9: Sample data for p-polarization at 1.0-9.5 GHz frequency range, incident angle 63.4°.

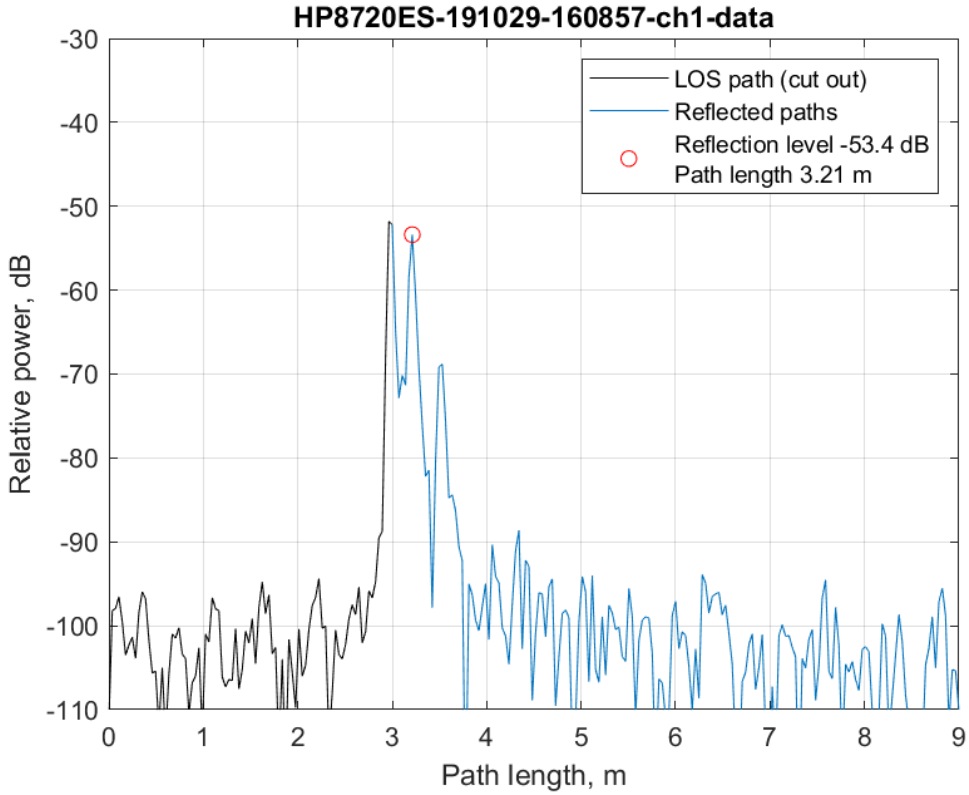

Figure 10: Sample data for s-polarization at 1-9.5 GHz frequency range, incident angle 66.6°.

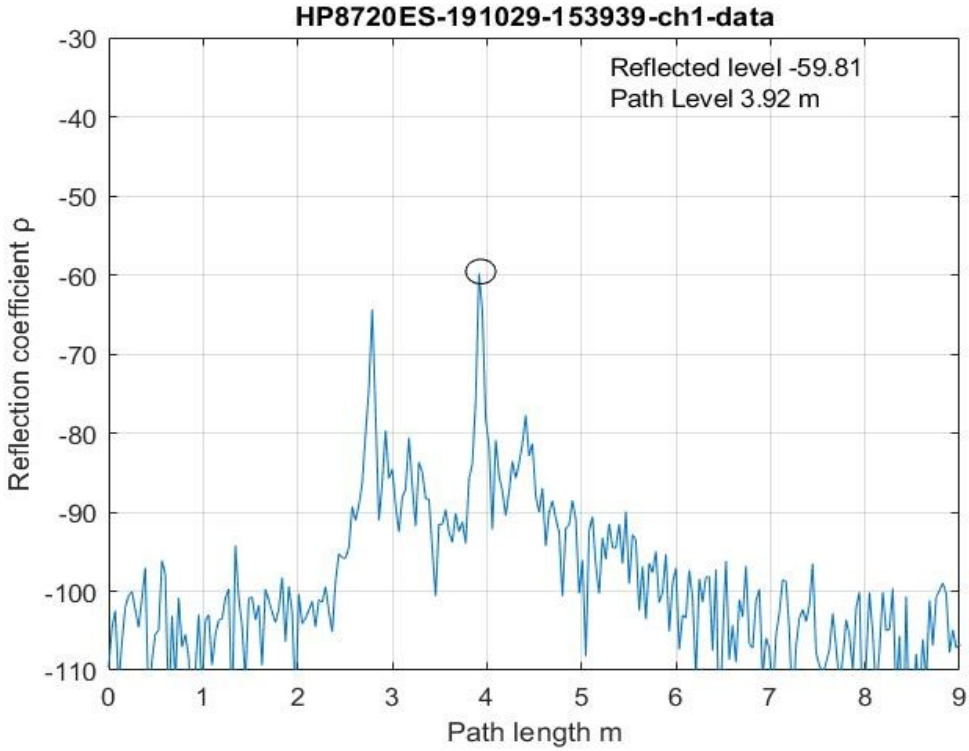

Figure 11: Sample data for p-polarization at 9.5-18 GHz frequency range, incident angle 43.8°.

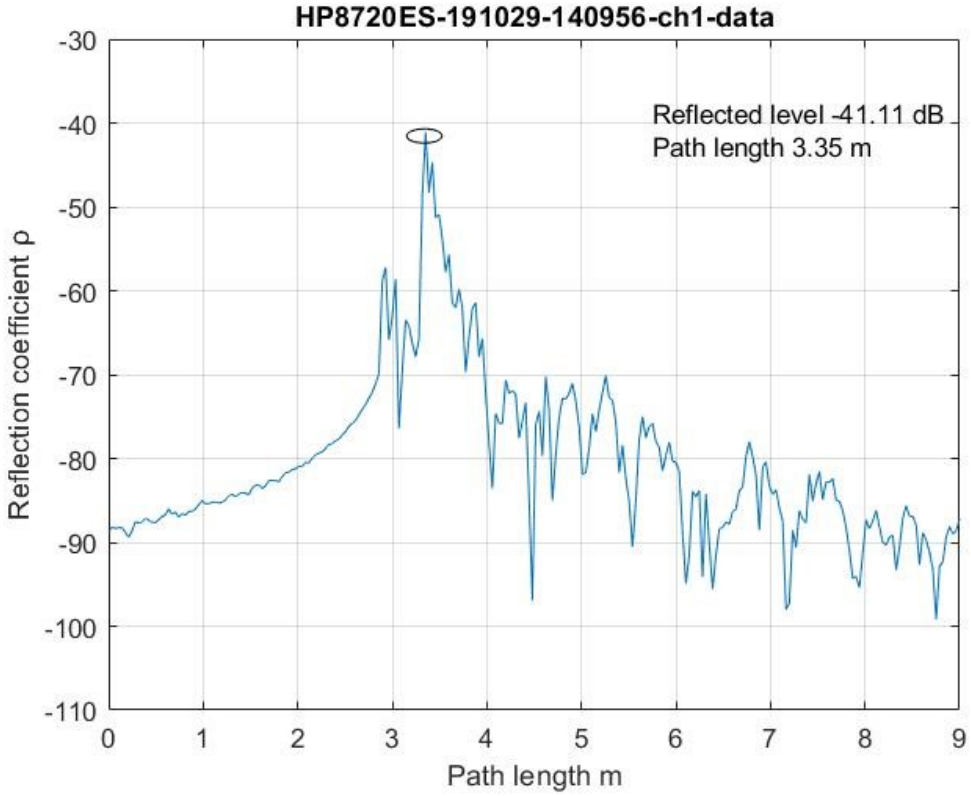

Figure 12: Sample data for s-polarization at 9.5-18 GHz frequency range, incident angle 58.7°.

The reflection coefficient is calculated as the difference of the received reflection path power level with respect to the LOS path power, both expressed in dB scale, and converted in the linear scale by transform $10^{(P_{REFL}-P_{LOS})/10}$.
The estimate for the complex dielectric constant is found by fitting the theoretical reflection coefficient curve (Eq. 38) in the p-polarization data and using minimum root mean square error (RMSE) as the fitting criterion. RMSE is calculated as

$$\text{RMSE} = \sqrt{\frac{1}{n}\sum_{i=1}^{n}\left(Y_i - \hat{Y}_i\right)^2}, \tag{38}$$

where Y_i is the sample value, $\hat{Y}_i$ is the estimation value, and n is the number of sample values [36].

The p-polarization reflection coefficient graphs for frequency ranges 1-18 GHz, 1.0-9.5 GHz and 9.5-18 GHz are given in Figures 13, 14 and 15, respectively. The reflection coefficients calculated from the measured data without path length compensation are represented by black dots.
Path length compensation considers the free space loss due longer propagation path. Compensation factor is according to [4]:

$$|\rho| = \frac{d_{refl}}{d_{los}}\sqrt{\frac{P_{refl}}{P_{refl}}} \tag{39}$$

After applying the path length compensation, coefficients falling within one degree from each other are averaged to give the data equal weighing over the abscissa. The average reflection coefficients are plotted with red markers. Finally, the theoretical curve of the reflection coefficient is fitted on the data.

The results are presented in Table 2.

Table 2: Complex relative permittivity of dry 19 mm plywood

	$\boldsymbol{\varepsilon_r = \varepsilon' - j\varepsilon''}$	**RMSE**
1-18 GHz	$2.13 - j0.78$	0.014
1-9.5 GHz	$1.90 - j0.79$	0.012
9.5-18 GHz	$2.35 - j0.58$	0.011

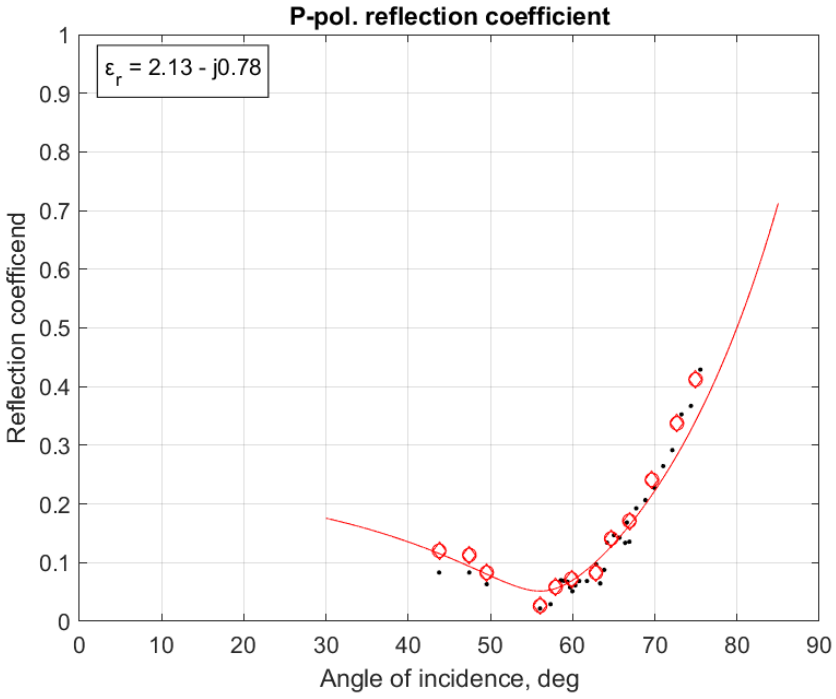

Figure 13: Reflection coefficient graph for p-polarization at 1-18 GHz frequency range.

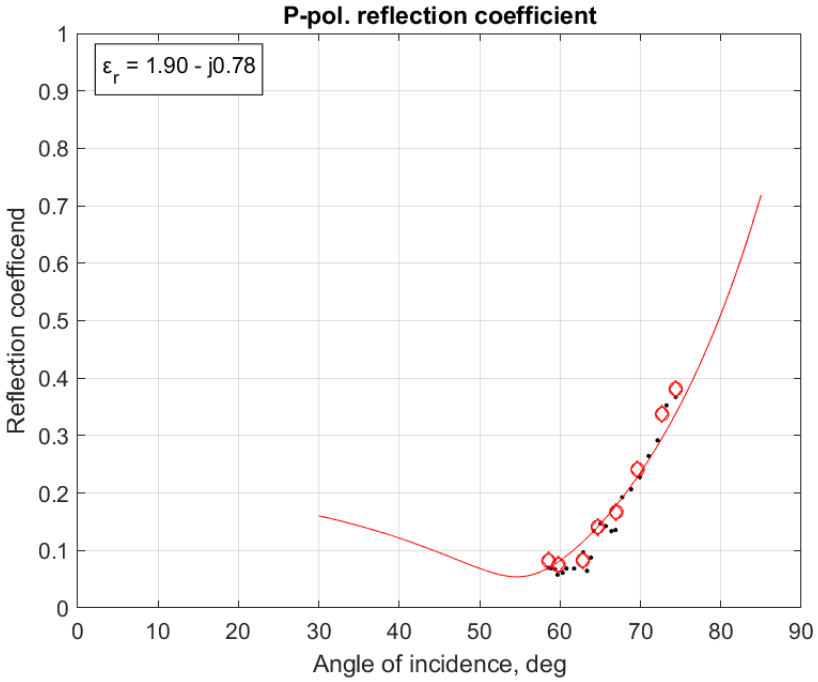

Figure 14: Reflection coefficient graph for p-polarization at 1.0-9.5 GHz frequency range.

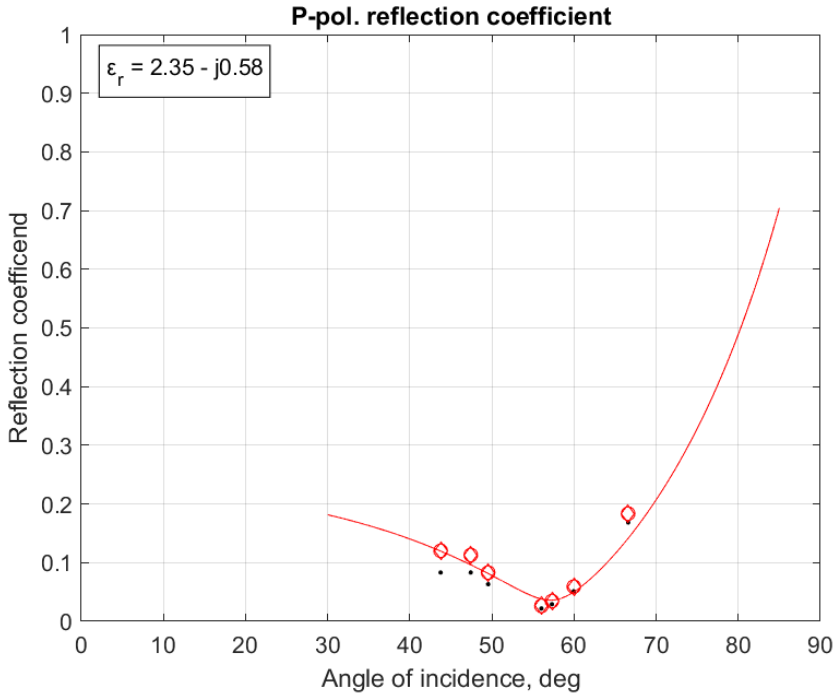

Figure 15: Reflection coefficient graph for p-polarization at 9.5-18 GHz frequency range.

7. DISCUSSION

7.1. Evaluation of the proposed model

After completing the measurement setup, the data is collected and analyzed. Figures 13, 14 and 15 shows the reflection coefficients against the incidence angles which gives the dielectric constant including the complex value. Table 2 shows the results. Observing the above scenarios, one can take the decision that the assessment process can provide the desired results. Finally, it can be said that the experiment is successfully done. However, the data recorded at lower frequency band has no samples below 58° angle of incidence, which leads to a rather low ε_r value. This is also evident in Figure 14.

7.2. Possible improvements for future work

There are several ways to improve the measurement system. Adding new options to the measurement system and reducing the operating time of sweeps can be a good improvisation. An external analysis software can be made and can be used for making the results smoother in the future. The measurement is not limited only into an anechoic chamber, but can be extended a fixed boundary like in a classroom or in outdoor environments. Using higher gain antennas are required only for setups where the reflation paths are longer. 10.5 dB horn antennas are enough to reach the required dynamic range in the current setup. More advanced graphical user interfaces can be used, instead of MATLAB. 4-port VNA and cross-polarized antennas enable measuring of both the p- and s-polarizations simultaneously.

8. SUMMARY

The goal of this thesis is to corroboration of a measurement setup for assessing dielectric constant. The measurement setup is designed by a two port VNA and two horn antennas. The setup is controlled, and data is collected by a control software. The system is efficient for operating in 1-18 GHz frequency range. This study relates to the propagation of electromagnetic wave and various affected phenomena during propagation. The theoretical part is basically concerning the propagation nature and impairments of electromagnetic wave and the effect of dielectric properties of dielectric materials when the electromagnetic wave is reflecting from the flat surface of a material sample. The experiments are done in an anechoic chamber and a dielectric material is placed between the TX and RX antennas in such a way that the angle of incidence can be varied in the reflection interaction. Various scenarios are created during the experiments and their results are evaluated. These results show the reflection coefficient and from the reflection coefficient the pseudo Brewster angle is determined. Finally, the assessment of complex dielectric constant is done with the help of Brewster angle and reflection coefficient.

9. REFERENCES

[1] K. R. Sturley, "Radio technology," *Encyclopeadia Britannica,* p. 1, 20 September 2019.

[2] keysight technologies, "number of points," 2000. [Online]. Available: http://na.support.keysight.com/vna/help/latest/S1_Settings/DPoints.htm. [Accessed 4 november 2019].

[3] V. Ivan, B. Niksa and N. Robert, "Estimation of dielectric constant of composite materials in buildings using reflected fields and PSO algorithm," in *Antennas and Propagation, EuCAP, European Conference on*, Barcelona, Spain, 2010.

[4] A. Regmi, *Reflection measurement of building materials at microwaves,* Oulu, 2016.

[5] R. Afzalzadeh, "Dielectric constant measurements of finite-size sheet at microwave frequencies by pseudo-Brewster's angle method," *IEEE Transactions on Microwave Theory and Techniques,* vol. 46(9), pp. 1307-1309, 1998.

[6] Openstax, J. L. Samuel, M. William and S. Jeff, University Physics Volume 2, Houston, Texas: OpenStax, 2016.

[7] J. S. Seybold, "Line-of-Sight Propagation and the Radio Horizon," in *Introduction to RF propagation*, New Jersey, John Wiley & Sons, Inc., 2005, p. 3.

[8] L. Barclay, "Propagation of radio waves," in *Reflection From Plane Surface*, London,, The Institution of Engineering and Technology, 2003, p. 88.

[9] A. Saakian, Radio wave propagation fundamentals, Artech House, 2017.

[10] Physclips, "Diffraction from a single slit. Young's experiment with finite slits.," The Australian learning and teaching council, [Online]. Available: https://www.animations.physics.unsw.edu.au/jw/light/single-slit-diffraction.html. [Accessed 11 November 2019].

[11] C. S. Baird, "Absorption of electromagnetic radiation," Mcgraw-hill global education holdings, llc., 09 2019. [Online]. Available: https://www.accessscience.com/content/absorption-of-electromagnetic-radiation/001600. [Accessed 14 12 2019].

[12] J. Sankar, "Antenna Polarisation," electronicsforu.com, 15 August 2016. [Online]. Available: https://electronicsforu.com/resources/learn-electronics/antenna-polarisation. [Accessed 27 September 2019].

[13] R. Fitzpatrick, "Polarization of Electromagnetic Waves," 8 April 2013. [Online]. Available: http://farside.ph.utexas.edu/teaching/315/Waves/node50.html. [Accessed 2019].

[14] A. Technologies, "Scattering of Electromagnetic Waves by Particles," AltaSim Technologies, 13 april 2013. [Online]. Available:

https://www.altasimtechnologies.com/electromagnetics/scattering-of-electromagnetic-waves-by-particles/. [Accessed 25 September 2019].

[15] F. Rana, "Electromagnetic Scattering," Cornell University, New york, 2007.

[16] R. L. Freeman, "Loss in Free Space," in *Radio System Design for Telecommunication*, New Jersey, John Wiley & Sons, Inc., 2007, p. 3.

[17] T. E. o. E. Britannica, "Encyclopædia Britannica," 16 December 2011. [Online]. Available: https://www.britannica.com/science/dielectric. [Accessed 18 August 2019].

[18] E. Tutorials, "Capacitance and Charge," AspenCore, Inc. , 2019. [Online]. Available: https://www.electronics-tutorials.ws/capacitor/cap_4.html. [Accessed 17 August 2019].

[19] P. B. Components, "The dielectric constant and its effects on the properties of a capacitor," EPCI (European Passive Components Institute), 2019. [Online]. Available: https://passive-components.eu/the-dielectric-constant-and-its-effects-on-the-properties-of-a-capacitor/. [Accessed 21 August 2019].

[20] C. R. Hong and O. Buyukozturk, "“Electromagnetic Properties of Concrete at," American Concrete Institute, 1998.

[21] M. C. Simon and K. V. Gottschalk, "Brewster angle in dielectric birefringent media: an explanation by means of dipolar model," *Optics communications,* vol. 126, no. 1-3, pp. 113-122, 1996.

[22] J. O. Smith, Physical audio signal processing for virtual musical instruments and audio effects, Julius O. Smith III, 2019.

[23] J. S. Seybold, " The Indoor Environment," in *Introduction to RF Propagation*, New Jersey, John Wiley & Sons, Inc., 2005, p. 209.

[24] D. I. Laurenson, "Indoor Radio Channel Propagation Modelling by Ray Tracing Techniques," 1994.

[25] E. Affum, E. Tchao, K. Diawuo and K. Agyekum, "Wideband Parameters Analysis and Validation for Indoor radio Channel at 60/70/80GHz for Gigabit Wireless Communication employing Isotropic, Horn and Omni directional Antenna," *International Journal of Advanced Computer Science and Applications,* pp. 292-297, 2013.

[26] A. Botonjic, "MIMO channel models," Institutionen för teknik och naturvetenskap, 2004.

[27] A. Zanella and R. Verdone, Pervasive Mobile and Ambient Wireless Communications: COST action 2100, Springer Science & Business Media, 2012.

[28] K. Technologies, "Basics of Measuring the Dielectric Properties of Materials," 2019.

[29] Newelectronics, "Six techniques for measuring dielectric properties," Newelectronics, 9 March 2017. [Online]. Available: http://www.newelectronics.co.uk/electronics-technology/six-techniques-for-measuring-dielectric-properties/152591/. [Accessed 3 November 2019].

[30] M. K. Alam, Electrical and Electronic Properties of Materials, London: Intechopen limited, 2019.

[31] M. R. Vanja, . R. Slavko and S. Mario, "Measuring the Dielectric Constant of Paper Using a Parallel Plate Capacitor," *International Journal of Electrical and Computer Engineering Systems,* vol. 9, pp. 1-10, 2018.

[32] G. Simpson, "Vector network analysis and ARFTG: A historical perspective," *50th ARFTG Conference Digest,* vol. 32, pp. 41-41, 1997.

[33] K. Technologies, "8720ES S-parameter Network Analyzer, 50 MHz to 20 GHz," Keysight Technologies, 2000-2019. [Online]. Available: https://www.keysight.com/en/pd-1000002256%3Aepsg%3Apro-pn-8720ES/s-parameter-network-analyzer?cc=US&lc=eng. [Accessed 27 October 2019].

[34] R. &. Schwarz, "R&S®HF906 Antenna," Rohde & Schwarz Hong Kong Limited, july 2006. [Online]. Available: https://www.rohde-schwarz.com/hk/product/hf906-productstartpage_63493-9337.html?rusprivacypolicy=0. [Accessed 27 october 2019].

[35] Microwaves101, "S-parameters," Microwaves101, 2001. [Online]. Available: https://www.microwaves101.com/encyclopedias/s-parameters. [Accessed 11 November 2019].

[36] B. Sridhar and M. Z. A. Khan, "RMSE comparison of path loss models for UHF/VHF bands in India," *2014 IEEE region 10 symposium,* pp. 330-335, 15 01 2014.